

Detecting correlation functions of ultracold atoms through Fourier sampling of time-of-flight images

L.-M. Duan

FOCUS center and MCTP, Department of Physics, University of Michigan, Ann Arbor, MI 48109

We propose a detection method for ultracold atoms which allows reconstruction of the full one-particle and two-particle correlation functions from the measurements. The method is based on Fourier sampling of the time-of-flight images through two consecutive impulsive Raman pulses. For applications of this method, we discuss a few examples, including detection of phase separation between superfluid and Mott insulators, various types of spin or superfluid orders, entanglement, exotic or fluctuating orders.

PACS numbers: 03.75.Ss, 05.30.Fk, 34.50.-s

Ultracold atomic gas provides an ideal system for controlled study of various kinds of strongly correlated many-body physics [1, 2, 3]. To reveal different many-body phenomena, the correlation function plays a critical role. In condensed matter systems, information about the correlation function is typically collected through linear response or scattering experiments [4]. For ultracold atomic gas, the most powerful detection technique is arguably the time-of-flight imaging [5]. For ballistic expansion of the atomic gas, the time-of-flight images actually give information of the atom number distribution in the momentum space, which corresponds to the diagonal terms of the one-particle correlation function. As we have only diagonal correlation function in the momentum space, it is in general inadequate to use it to reconstruct the correlation function in the real space.

In this paper, we propose a detection method which extends the time-of-flight imaging technique by gaining much more information of the correlation function. The method detects all the non-diagonal correlation terms as well as the diagonal ones in the momentum space through application of two consecutive impulsive Raman pulses at the beginning of the expansion which introduces a tunable momentum difference to the correlation terms. With this kind of Fourier sampling in the momentum space, one can reconstruct the full one-particle correlation function in the real space. If one repeats the time-of-flight imaging measurements many times, as has been shown in recent works [6, 7], it is also possible to detect the noise spectroscopy by looking at the statistical correlation between different images. With a combination of the Fourier sampling and the noise spectroscopy, one can also reconstruct the full two-particle correlation function. The reconstruction of the full one-particle and two-particle correlation functions represents an unprecedented detection ability, which gives very detailed information of the underlying many-body system. As illustration of applications, we discuss a few examples, including detection of phase separation between the superfluid and the Mott insulator states for bosonic atoms in a trap, various types of spin or superfluid orders in multi-component Bose or fermi gas, entanglement in an optical lattice, patterns of the valence bonds associated with some exotic

quantum phases [9], and the fluctuating orders which exist only in short distance [10].

In the time-of-flight imaging experiment, what one measures from light absorption is the column integrated density of the expanding atomic cloud. The signal is proportional to the column average of the atom density operator, which, for the spin component α , is denoted as $\langle n_\alpha(\mathbf{r}, t) \rangle = \langle \Psi_\alpha^\dagger(\mathbf{r}, t) \Psi_\alpha(\mathbf{r}, t) \rangle$, where $\Psi_\alpha(\mathbf{r}, t)$ represents the field operator for bosonic or fermionic atoms at the position \mathbf{r} and the expansion time t . We assume ballistic expansions with the atomic collision effect negligible during the time of flight [11]. In such a case, if the expansion time t is long enough so that the size of the final expanded cloud is much larger than the size of the initial one, the density $\langle n_\alpha(\mathbf{r}, t) \rangle$ is connected with the initial momentum distribution of the atoms by a simple relation $\langle n_\alpha(\mathbf{r}, t) \rangle \propto \langle n_\alpha(\mathbf{k}) \rangle = \langle \Psi_\alpha^\dagger(\mathbf{k}) \Psi_\alpha(\mathbf{k}) \rangle$ with the corresponding wave vector $\mathbf{k} = m\mathbf{r}/(\hbar t)$ [5, 6]. So the conventional time-of-flight imaging measures the diagonal terms of the one-particle correlation function in the momentum space.

To reconstruct the full one-particle correlation function, it is required to measure also the non-diagonal correlation terms $\langle \Psi_\alpha^\dagger(\mathbf{k}) \Psi_\alpha(\mathbf{k}') \rangle$ in the momentum space. For that purpose, we propose a detection method as illustrated in Fig. 1, which combines the time-of-flight imaging with two consecutive impulsive Raman pulses. We assume there is an additional atomic hyperfine spin level β which is initially empty (such a level is always available for typical alkali atoms). Right after turnoff of the trapping potential but before any significant expansion of the atomic cloud, we apply two impulsive Raman pulses to all the atoms. The duration δt of the Raman pulses is short so that one can neglect the cloud expansion and the atomic collision within δt . We assume that the two travelling-wave beams for the first Raman operation are propagating along different directions with the corresponding wave vectors \mathbf{k}_1 and \mathbf{k}_2 , so the effective Raman Rabi frequency has a spatially varying phase with the form $\Omega(\mathbf{r}) = \Omega_0 e^{i(\delta\mathbf{k}\cdot\mathbf{r} + \varphi_1)}$, where $\delta\mathbf{k} \equiv \mathbf{k}_2 - \mathbf{k}_1$ and φ_1 is a constant phase. The Hamiltonian within the interval δt can then be written as $H = \int d^3\mathbf{r} \Omega(\mathbf{r}) \Psi_\alpha^\dagger(\mathbf{r}) \Psi_\beta(\mathbf{r}) + H.c.$ Transferring this

Hamiltonian into the momentum space, we have

$$H = \sum_{\mathbf{k}} \Omega_0 e^{i\varphi_1} \Psi_{\alpha}^{\dagger}(\mathbf{k}) \Psi_{\beta}(\mathbf{k} + \delta\mathbf{k}) + H.c. \quad (1)$$

We choose the intensity of the Raman beams so that $\Omega_0 \delta t = \pi/4$. After this Raman operation, the final field operators in the momentum space, denoted as $\Psi'_{\alpha}(\mathbf{k})$ and $\Psi'_{\beta}(\mathbf{k})$, are connected with the initial ones $\Psi_{\alpha}(\mathbf{k}), \Psi_{\beta}(\mathbf{k})$ through the relation

$$\begin{aligned} \Psi'_{\alpha}(\mathbf{k}) &= [\Psi_{\alpha}(\mathbf{k}) + e^{i\varphi_1} \Psi_{\beta}(\mathbf{k} + \delta\mathbf{k})] / \sqrt{2}, \\ \Psi'_{\beta}(\mathbf{k}) &= [\Psi_{\beta}(\mathbf{k}) - e^{-i\varphi_1} \Psi_{\alpha}(\mathbf{k} - \delta\mathbf{k})] / \sqrt{2}. \end{aligned} \quad (2)$$

Then, we immediately apply the second Raman operation which is from two co-propagating laser beams connecting the levels α, β with a spatially constant effective Rabi frequency $\Omega_0 e^{i\varphi_2}$. With the same pulse area $\Omega_0 \delta t = \pi/4$, the second Raman operation induces the transformation

$$\begin{aligned} \Psi''_{\alpha}(\mathbf{k}) &= [\Psi'_{\alpha}(\mathbf{k}) + e^{i\varphi_2} \Psi'_{\beta}(\mathbf{k})] / \sqrt{2}, \\ \Psi''_{\beta}(\mathbf{k}) &= [\Psi'_{\beta}(\mathbf{k}) - e^{-i\varphi_2} \Psi'_{\alpha}(\mathbf{k})] / \sqrt{2}, \end{aligned} \quad (3)$$

where $\Psi''_{\alpha}(\mathbf{k}), \Psi''_{\beta}(\mathbf{k})$ denote the final field operators after the second Raman operation. We then perform the conventional time-of-flight imaging, with the atoms in different spin components α, β separated during the flight through a magnetic field gradient [5]. This imaging measures the momentum distribution $\langle n''_{\alpha}(\mathbf{k}) \rangle = \langle \Psi''_{\alpha}{}^{\dagger}(\mathbf{k}) \Psi''_{\alpha}(\mathbf{k}) \rangle$ and $\langle n''_{\beta}(\mathbf{k}) \rangle = \langle \Psi''_{\beta}{}^{\dagger}(\mathbf{k}) \Psi''_{\beta}(\mathbf{k}) \rangle$. With a combination of Eqs. (2) and (3), we find that the difference between the two images $\langle n''_{\alpha\beta}(\mathbf{k}) \rangle \equiv \langle n''_{\alpha}(\mathbf{k}) \rangle - \langle n''_{\beta}(\mathbf{k}) \rangle$ gives the non-diagonal correlation terms

$$\langle n''_{\alpha\beta}(\mathbf{k}) \rangle = -\text{Re} \langle \Psi_{\alpha}^{\dagger}(\mathbf{k}) \Psi_{\alpha}(\mathbf{k} - \delta\mathbf{k}) e^{i\delta\varphi} \rangle, \quad (4)$$

where $\delta\varphi = \varphi_2 - \varphi_1$ and we have used the fact that $\Psi_{\beta}(\mathbf{k})$ is initially in the vacuum state.

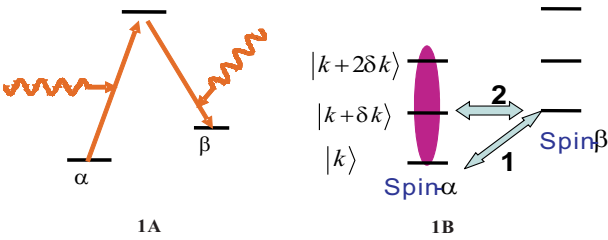


FIG. 1: (1A) Raman pulses with different propagating directions introduce a momentum kick. (1B) The momentum ladder connected by two consecutive impulsive Raman pulses. The first $\pi/2$ Raman pulse (pulse 1) introduces a tunable momentum kick δk , while the second one (pulse 2) has no kick. The atoms are initially in the spin- α state.

With the above method, we have shown how to measure the real and imaginary parts of the non-diagonal correlation function $\langle \Psi_{\alpha}^{\dagger}(\mathbf{k}) \Psi_{\alpha}(\mathbf{k} - \delta\mathbf{k}) \rangle$ by

choosing the relative phase $\delta\varphi = \mathbf{0}$ or $\pi/2$, respectively. The momentum difference $\delta\mathbf{k}$ is controlled by the relative angle of the two laser pulses for the first Raman operation. By varying this angle, $\delta\mathbf{k}$ can be varied from 0 to $2\mathbf{k}_0$, where $|\mathbf{k}_0| = 2\pi/\lambda$ is the optical wave vector. With a Fourier transform of $\langle \Psi_{\alpha}^{\dagger}(\mathbf{k}) \Psi_{\alpha}(\mathbf{k} - \delta\mathbf{k}) \rangle$, one can reconstruct the real-space correlation function $\langle \Psi_{\alpha}^{\dagger}(\mathbf{r} + \delta\mathbf{r}/2) \Psi_{\alpha}(\mathbf{r} - \delta\mathbf{r}/2) \rangle = \int \langle \Psi_{\alpha}^{\dagger}(\mathbf{k} + \delta\mathbf{k}/2) \Psi_{\alpha}(\mathbf{k} - \delta\mathbf{k}/2) \rangle e^{i(\mathbf{k} \cdot \delta\mathbf{r} + \delta\mathbf{k} \cdot \mathbf{r})} d\delta\mathbf{k} d\mathbf{k} / 2\pi$, with a spatial resolution in \mathbf{r} down to $2\pi/|\delta\mathbf{k}|_{\text{max}} = \lambda/2$. This kind of Fourier sampling in the momentum space through the laser phase gradient allows us to directly probe very small spatial structure in the ultracold atomic gas, although the probe beams are always shined on all the atoms without separate addressing of any particular region. For instance, for the case of atoms in an optical lattice, with such a resolution, we can reconstruct the correlation $\langle a_{\alpha}^{\dagger}(i) a_{\alpha}(j) \rangle$ of the mode operators a_{α} at two arbitrary sites i and j (the lattice spacing is $\lambda/2$).

Before showing how to measure the full two-particle correlation function, we add a few remarks here. First, note that in the above method, it is essential to apply two consecutive Raman operations. If we introduce momentum difference $\delta\mathbf{k}$ by applying only one Raman operation on the same spin component α with the Hamiltonian $H' = \sum_{\mathbf{k}} \Omega_0 e^{i\varphi_1} \Psi_{\alpha}^{\dagger}(\mathbf{k}) \Psi_{\alpha}(\mathbf{k} + \delta\mathbf{k}) + H.c.$, the H' will couple the whole momentum ladder $\Psi_{\alpha}(\mathbf{k}), \Psi_{\alpha}(\mathbf{k} \pm \delta\mathbf{k}), \Psi_{\alpha}(\mathbf{k} \pm 2\delta\mathbf{k}), \dots$, and we thus cannot get a simple form of transformation such as those given by Eqs. (2) and (3). So the method with two consecutive Raman operations seems to be the easiest one for measuring the non-diagonal momentum correlations. Second, in the above method, we have assumed to tune the momentum difference by changing the relative angle of two laser pulses. This tuning can also be achieved by applying a sequence of laser pulses incident along two fixed directions with a small angle $\delta\theta$, with each pair of pulses introducing a fixed momentum kick $\mathbf{k}_{\delta} = 2|\mathbf{k}_0| \sin(\delta\theta/2) \simeq |\mathbf{k}_0| \delta\theta$ (see illustration in Fig. 2 and its caption). With a maximum of N such pulse pairs, the momentum difference $\delta\mathbf{k}$ in the correlation function (4) can be tuned among different values $\mathbf{k}_{\delta}, 2\mathbf{k}_{\delta}, \dots, N\mathbf{k}_{\delta}$, which corresponds to a discrete Fourier sampling of the atomic correlation function with the momentum-space and real-space resolutions given respectively by $|\mathbf{k}_0| \delta\theta$ and $\lambda/(N\delta\theta)$. Finally, the above method can be generalized straightforwardly to measure also the spin-spatial correlations. If we have multiple Zeeman spin components α, α', \dots for the state of the atomic cloud, one can reconstruct the full spin-spatial correlation $\langle \Psi_{\alpha}^{\dagger}(\mathbf{k}_1) \Psi_{\alpha'}(\mathbf{k}_2) \rangle$ (or $\langle \Psi_{\alpha}^{\dagger}(\mathbf{r}_1) \Psi_{\alpha'}(\mathbf{r}_2) \rangle$) through a combination of the above Fourier sampling with a pair of Raman pulses which mixes the spin components α, α' .

The above method, combined with the noise spectroscopy, can also be used to reconstruct the full two-particle correlation function $\langle \Psi_{\alpha}^{\dagger}(\mathbf{r}_1) \Psi_{\alpha}^{\dagger}(\mathbf{r}_2) \Psi_{\alpha}(\mathbf{r}_3) \Psi_{\alpha}(\mathbf{r}_4) \rangle$. For the noise spectroscopy [6, 7], one just needs to note that for different runs of experiment, the time-of-flight images can have

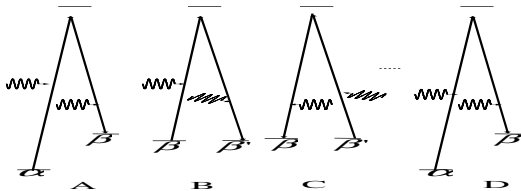


FIG. 2: Tunable momentum kicks with pulses propagating in fixed directions. Steps (A) and (D) represent $\pi/2$ pulses with no momentum kicks. Steps (B) and (C) represent π pulses which a small fixed momentum kick k_δ (pulses for B, C are propagating in reverse directions). The intermediate pulses B, C can be applied with a controlled number of times, which correspond a discrete Fourier sampling of the correlation function with a momentum-space resolution of k_δ .

quantum fluctuation even if one starts with the same state of the atomic cloud. One image corresponds to a single-run measurement of the column integrated atomic density operator, and by looking at correlation of different images, one can find out quantum correlation of the density operator. To detect such quantum correlation, all the technical noise for the images needs to be reduced below the level of quantum noise. It is remarkable that the recent experiments have shown that such quantum correlation of images is indeed visible after suppression of the technical noise [7]. Each time-of-flight imaging corresponds to a measurement of the one-particle momentum correlation $\langle \Psi_\alpha^\dagger(\mathbf{k}) \Psi_\alpha(\mathbf{k} - \delta\mathbf{k}) \rangle$. To reconstruct the full two-particle correlation function, one just needs to repeat each of such imaging measurements M times (M needs to be sufficiently large so that $1/\sqrt{M}$, which characterize the statistical error for the quantum correlation measurement, is sufficiently small). Then, by looking at the correlation of arbitrary two images corresponding to $\langle \Psi_\alpha^\dagger(\mathbf{k}) \Psi_\alpha(\mathbf{k} - \delta\mathbf{k}) \rangle$ and $\langle \Psi_\alpha^\dagger(\mathbf{k}') \Psi_\alpha(\mathbf{k}' - \delta\mathbf{k}') \rangle$ respectively, one gets the two-particle correlation $\langle \Psi_\alpha^\dagger(\mathbf{k}) \Psi_\alpha(\mathbf{k} - \delta\mathbf{k}) \Psi_\alpha^\dagger(\mathbf{k}') \Psi_\alpha(\mathbf{k}' - \delta\mathbf{k}') \rangle$. As the two images can be arbitrarily chosen (with different $\mathbf{k}, \mathbf{k}', \delta\mathbf{k}, \delta\mathbf{k}'$), this gives us the full two-particle correlation in the momentum space, and the real-space correlation $\langle \Psi_\alpha^\dagger(\mathbf{r}_1) \Psi_\alpha(\mathbf{r}_2) \Psi_\alpha^\dagger(\mathbf{r}_3) \Psi_\alpha(\mathbf{r}_4) \rangle$ is simply its Fourier transform. The spatial resolution in this case is still given by $\lambda/2$ similar to the one-particle correlation measurement.

The measurement of the full one-particle and two-particle correlation functions gives very detailed information of the many-body properties of the underlying system. Here, we give a few examples for illustration of its applications. We start with one-particle correlation function. As the first example, note that for the superfluid to Mott insulator transition in a global harmonic trap (as it is the case for experiments), theory has predicted phase separation with layers of superfluid states intervened in by layers of Mott insulator states with decreasing integer filling numbers [8]. Such a picture

have not been confirmed yet by experiments as with the conventional time-of-flight imaging, it is hard to see this layer-by-layer structure. Through the Fourier sampling, however, one can reconstruct the one-particle correlation $\langle \Psi_\alpha^\dagger(\mathbf{r}_1) \Psi_\alpha(\mathbf{r}_2) \rangle$. From this correlation, it would be evident to see the phase separation: the Mott insulator state is characterized by a vanishing non-diagonal correlation and a constant (integer) diagonal correlation, while the superfluid state is characterized by both non-zero diagonal and non-diagonal correlations which vary continuously in space.

With ultracold atoms in an optical lattice, one can realize different magnetic Hamiltonians [12]. Depending on the lattice geometry and interaction configurations, such Hamiltonians may support various types of magnetic orders [12, 13]. The magnetic orders typically can be written in the form $\langle \mathbf{S}_i \rangle = \mathbf{v}_1 \cos(\mathbf{K} \cdot \mathbf{r}_i) + \mathbf{v}_2 \sin(\mathbf{K} \cdot \mathbf{r}_i)$ [9], where \mathbf{S}_i is the spin operator on the site i with the coordinate \mathbf{r}_i , \mathbf{v}_1 and \mathbf{v}_2 are two vectors specifying certain directions, and \mathbf{K} characterizes spatial variation of the order parameter. The spin \mathbf{S}_i is defined as $\mathbf{S}_i = \sum_{\alpha\alpha'} a_{i\alpha}^\dagger \sigma_{\alpha\alpha'} a_{i\alpha'}/2$, where σ is the Pauli matrix and $a_{i\alpha}$ is the mode operator which is connected with the field operator $\Psi_\alpha(\mathbf{r})$ through $a_{i\alpha} = \int w_i^*(\mathbf{r}) \Psi_\alpha(\mathbf{r}) d^3\mathbf{r}$ ($w_i^*(\mathbf{r})$ is the Wannier function for the site i). Through Fourier sampling of the time-of-flight images with a resolution $\lambda/2$, one can reconstruct correlation of the mode operators $\langle a_{i\alpha}^\dagger a_{j\alpha'} \rangle$ on any sites ($i = j$ for the special case). So one can directly detect any type of spatial variation of the order parameter $\langle \mathbf{S}_i \rangle$ (note that the conventional time-of-flight imaging cannot detect spatially varying order parameters).

Another interesting application of this Fourier sampling technique is to detect local fluctuating orders. Local fluctuating orders, such as stripes (unidirectional density waves), have received wide attention in strongly correlated physics (in particular for high-Tc superconductors) [10]. The local fluctuating order typically takes place near a critical point with competing orders or at the proximity of an ordered phase. With ultracold fermions in an optical lattice, the fundamental Hamiltonian is very similar to those models for high-Tc superconductors [14, 15]. One expects that competing fluctuating orders may arise as well in the phase diagram of this system. The local fluctuating orders such as stripes correspond to real-space patterns of some micro-phase separation [10], and the conventional time-of-flight imaging cannot see it because it will be averaged out. However, through the Fourier sampling technique with a spatial resolution down to the lattice constant, it should be evident to detect these local fluctuating orders whenever they show up. A measurement of the one-particle correlation $\langle \Psi_\alpha^\dagger(\mathbf{r}_1) \Psi_{\alpha'}(\mathbf{r}_2) \rangle$ is typically enough to probe the fluctuating orders such as the local density waves (stripes).

The above discussion shows some applications of the one-particle correlation. With the two-particle correla-

tion measured, one can gain further information. For example, one can use the two-particle correlation to unambiguously detect the entanglement pattern for ultracold atoms in an optical lattice. Through controlled atomic collisions, one can generate entanglement for atoms on different lattice sites [16], and some initial experimental evidence of entanglement has been reported for such a system [17]. It is hard however to directly detect atomic entanglement between different sites or regions inside an optical lattice as the conventional detection technique do not have such a spatial resolution. This entanglement can be unambiguously confirmed with a measurement of spin correlations for atoms on different sites (similar to the Bell inequality measurement). As each spin operator involves only two atomic mode operators, the spin correlation is included in the two-particle correlation function. So, a measurement of the two-particle correlation can give information of spin entanglement pattern in the lattice.

For fermionic systems with pairing instability (such as the fermionic superfluid state [3]), it is also desirable to have a method to directly measure the Cooper pair function $\langle \Psi_\alpha(\mathbf{r}_1) \Psi_{\alpha'}(\mathbf{r}_2) \rangle$. The two-particle correlation also gives information of such pair function as with Cooper pairing, the two-particle correlation can be typically approximated with the following decomposition $\langle \Psi_\alpha^\dagger(\mathbf{r}_1) \Psi_{\alpha'}^\dagger(\mathbf{r}_2) \Psi_{\alpha'}(\mathbf{r}_3) \Psi_\alpha(\mathbf{r}_4) \rangle \approx \langle \Psi_\alpha^\dagger(\mathbf{r}_1) \Psi_{\alpha'}^\dagger(\mathbf{r}_2) \rangle \langle \Psi_{\alpha'}(\mathbf{r}_3) \Psi_\alpha(\mathbf{r}_4) \rangle + \langle \Psi_\alpha^\dagger(\mathbf{r}_1) \Psi_\alpha(\mathbf{r}_4) \rangle \langle \Psi_{\alpha'}^\dagger(\mathbf{r}_2) \Psi_{\alpha'}(\mathbf{r}_3) \rangle - \langle \Psi_\alpha^\dagger(\mathbf{r}_1) \Psi_{\alpha'}(\mathbf{r}_3) \rangle \langle \Psi_{\alpha'}^\dagger(\mathbf{r}_2) \Psi_\alpha(\mathbf{r}_4) \rangle$ by applying the Wick theorem. As the one-particle correlation is known already with the Fourier sampling, so a measurement of the two-particle correlation gives the pair function $\langle \Psi_\alpha(\mathbf{r}_1) \Psi_{\alpha'}(\mathbf{r}_2) \rangle$ (the two-particle correlation actually contains more information, for instance, it can be used to check self-consistently whether the above decomposition is valid). The pair function

$\langle \Psi_\alpha(\mathbf{r}_1) \Psi_{\alpha'}(\mathbf{r}_2) \rangle$ can tell us the symmetry (s-wave or d-wave for instance) and the size of the Cooper pairs as well as how the pair structure changes in space.

Finally, a potentially more interesting application of the two-particle correlation might be that it gives us a way to directly detect the patterns of valence bonds in an optical lattice. A valence bond on the sites i, j (not necessarily neighbors) is simply the ground state of the bond operator $Q_{ij} = \mathbf{S}_i \cdot \mathbf{S}_j$ (\mathbf{S}_i are spin operators) [9]. The resonating valence bond (RVB) states [9, 18], which include many possible patterns of the valence bond distribution in the lattice, have been conjectured as one of the most likely ground state of the t - J or Hubbard models in the strongly correlated limit. As the number of possible configurations of the RVB states increases exponentially with the size of the lattice, it is hard to figure out the distribution pattern of the valence bonds in a lattice. However, with an atomic realization of the t - J model [15], one can directly measure the bond operators Q_{ij} in an optical lattice to find out the most likely distribution pattern of the valence bonds. Each bond operator Q_{ij} corresponds to a special component of the two-particle correlation function, so a measurement of the two-particle correlation with Fourier sampling gives complete information about the bond distribution.

In summary, we have proposed a detection method which combines the commonly-used time-of-flight imaging technique with the Fourier sampling based on application of two consecutive impulsive Raman pulses. This detection method allows us to reconstruct the full one-particle and two-particle correlation functions. We have discussed a few examples for illustration of the wide applications of the correlation functions for probing many-body properties of the underlying system.

This work was supported by the NSF award (0431476), the ARDA under ARO contracts, and the A. P. Sloan Fellowship.

-
- [1] For a review, see D. Jaksch, P. Zoller, cond-mat/0410614.
[2] M. Greiner, et al., Nature 415, 39 (2002); C. Orzel, et al., Science 291, 2386 (2001).
[3] C.A. Regal, M. Greiner and D.S. Jin, Phys. Rev. Lett. **92**, 040403 (2004); M.W. Zwierlein *et al.*, Phys. Rev. Lett. **92**, 120403 (2004); C. Chin *et al.*, Science **305**, 1128 (2004); J. Kinast *et al.*, Science **307**, 1296 (2005); M.W. Zwierlein *et al.*, Nature 435, 1047 (2005); M. Holland *et al.*, Phys. Rev. Lett. **87**, 120406 (2001).
[4] W. Jones, and N. H. March, *Theoretical solid state physics*, Dove, New York (1985).
[5] For a review, see W. Ketterle, D.S. Durfee, D.M. Stamper-Kurn, cond-mat/9904034.
[6] E. Altman, E. Demler, M. D. Lukin, Phys. Rev. A 70, 013603 (2004).
[7] S. Folling et al., Nature 434, 481 (2005); M. Greiner et al., Phys. Rev. Lett. 94, 110401 (2005); C.-S. Chuu et al., quant-ph/0508143.
[8] D. Jaksch, et al., Phys. Rev. Lett. **81**, 3108 (1998); B. DeMarco et al., cond-mat/0501718.
[9] S. Sachdev, Rev. Mod. Phys. 75, 913 (2003).
[10] S.A. Kivelson et al., Rev. Mod. Phys. 75, 1201 (2003).
[11] For optical lattice experiments with small filling factors, the ballistic expansion is typically a good approximation. With the Feshbach resonance technique, one can also always tune the collision interaction to a negligible magnitude at the beginning of the expansion to satisfy the condition of the ballistic expansion.
[12] L.-M. Duan, E. Demler, M. D. Lukin, Phys. Rev. Lett. 91, 090402 (2003).
[13] L. Santos et al., Phys. Rev. Lett. 93, 030601 (2004).
[14] W. Hofstetter et al., Phys. Rev. Lett. 89, 220407 (2002).
[15] L.-M. Duan, cond-mat/0508745.
[16] D. Jaksch, et al., Phys. Rev. Lett. 82, 1975 (1999).
[17] O. Mandel et al., Nature 425, 937 (2003).
[18] P. W. Anderson, Science 235, 1196 (1987).